



**HAL**  
open science

## **Strong anharmonicity induces quantum melting of charge density wave in 2H-NbSe<sub>2</sub> under pressure**

Maxime Leroux, Ion Errea, Mathieu Le Tacon, Sofia-Michaela Souliou, Gaston Garbarino, Laurent Cario, Alexey Bosak, Francesco Mauri, Matteo Calandra, Pierre Rodière

► **To cite this version:**

Maxime Leroux, Ion Errea, Mathieu Le Tacon, Sofia-Michaela Souliou, Gaston Garbarino, et al.. Strong anharmonicity induces quantum melting of charge density wave in 2H-NbSe<sub>2</sub> under pressure. 2015. hal-01187238v1

**HAL Id: hal-01187238**

**<https://hal.science/hal-01187238v1>**

Preprint submitted on 26 Aug 2015 (v1), last revised 5 Nov 2015 (v2)

**HAL** is a multi-disciplinary open access archive for the deposit and dissemination of scientific research documents, whether they are published or not. The documents may come from teaching and research institutions in France or abroad, or from public or private research centers.

L'archive ouverte pluridisciplinaire **HAL**, est destinée au dépôt et à la diffusion de documents scientifiques de niveau recherche, publiés ou non, émanant des établissements d'enseignement et de recherche français ou étrangers, des laboratoires publics ou privés.

# Strong anharmonicity induces quantum melting of charge density wave in 2H-NbSe<sub>2</sub> under pressure

Maxime Leroux,<sup>1,\*</sup> Ion Errea,<sup>2,3,4</sup> Mathieu Le Tacon,<sup>5</sup> Sofia-Michaela Souliou,<sup>5</sup> Gaston Garbarino,<sup>6</sup> Laurent Cario,<sup>7</sup> Alexey Bosak,<sup>6</sup> Francesco Mauri,<sup>4</sup> Matteo Calandra,<sup>4,†</sup> and Pierre Rodière<sup>1,‡</sup>

<sup>1</sup>*Université Grenoble Alpes, CNRS, I. Néel, F-38000 Grenoble, France*

<sup>2</sup>*Donostia International Physics Center (DIPC), Manuel de Lardizabal Pasealekua 4, 20018 Donostia-San Sebastián, Basque Country, Spain*

<sup>3</sup>*IKERBASQUE, Basque Foundation for Science, 48011, Bilbao, Spain*

<sup>4</sup>*IMPMC, UMR CNRS 7590, Sorbonne Universités - UPMC Univ. Paris 06, MNHN, IRD, 4 Place Jussieu, F-75005 Paris, France*

<sup>5</sup>*Max-Planck-Institut für Festkörperforschung, Heisenbergstr. 1, D-70569 Stuttgart, Germany*

<sup>6</sup>*European Synchrotron Radiation Facility - Grenoble, France*

<sup>7</sup>*Institut des Matériaux Jean Rouxel (IMN), Université de Nantes, CNRS, 2 rue de la Houssinière, BP3229, 44322 Nantes, France*

(Dated: August 26, 2015)

The interplay between charge density wave (CDW) order and superconductivity has attracted much attention. This is the central issue of a long standing debate in simple transition metal dichalcogenides without strong electronic correlations, such as 2H-NbSe<sub>2</sub>, in which two such phases coexist. The importance of anisotropic electron-phonon interaction has been recently highlighted from both theoretical and experimental point of view, and explains some of the key features of the formation of the CDW in this system. On the other hand, other aspects, such as the effects of anharmonicity, remain poorly understood despite their manifest importance in such soft-phonon driven phase transition. At the theoretical level in particular, their prohibitive computational price usually prevents their investigation within conventional perturbative approaches.

Here, we address this issue using a combination of high resolution inelastic X-ray scattering measurements of the phonon dispersion, as a function of temperature and pressure, with state of the art ab initio calculations. By explicitly taking into account anharmonic effects, we obtain an accurate, quantitative, description of the (P,T) dependence of the phonon spectrum, accounting for the rapid destruction of the CDW under pressure by zero mode vibrations - or quantum fluctuations - of the lattice. The low-energy longitudinal acoustic mode that drives the CDW transition barely contributes to superconductivity, explaining the insensitivity of the superconducting critical temperature to the CDW transition.

## I. INTRODUCTION

The transition metal dichalcogenide 2H-NbSe<sub>2</sub> is a material with weak electron-electron correlations that un-

dergoes, at ambient pressure and  $T_{CDW}=33.5$  K, a second order phase transition towards an incommensurate CDW phase, i.e. a static modulation of the electronic density close to the Fermi level<sup>1,2</sup>. The anisotropy and temperature dependence of the electronic band structure has been widely studied by ARPES and STM measurements<sup>3-9</sup>. The CDW is coupled to a periodic lattice distortion through a strong electron-phonon coupling. The transition is associated with a softening of a longitudinal acoustic phonon mode as temperature is lowered to  $T_{CDW}$ <sup>10</sup>. Below  $T_c = 7.2$  K, the CDW further coexists with superconductivity.

By applying an hydrostatic pressure,  $T_{CDW}$  is driven to 0 K and the CDW instability disappears above the critical pressure  $P_{CDW}(T = 3.5 \text{ K})=4.6$  GPa<sup>11</sup>. Around this quantum phase transition superconductivity remains essentially unaffected, as shown on the (T,P) phase diagram in Fig. 1<sup>12,13</sup>.

At ambient pressure, published ab initio calculations reproduce successfully the lattice instability on a wide part of the Brillouin zone around the experimentally observed  $\mathbf{q}_{CDW}$ <sup>10,14,15</sup>. However, these calculations are carried out at the harmonic level, and therefore at T=0K. The temperature dependence can be qualitatively reproduced using a Gaussian smearing of the Fermi surface which wipes out the contribution of the electron-phonon interaction. Quantitatively however, the temperatures that would effectively yield this smearing are unphysical, as they exceed the experimentally observed one by several orders of magnitude. Moreover, even for T=0 K, harmonic ab initio calculations as a function of pressure (see SI and <sup>16</sup>) predict (see Fig. 3 and SI) a CDW instability up to  $P_C = 14$  GPa, a pressure that largely exceeds the experimentally observed one of  $P_{CDW} = 4.6$  GPa. This persistence of the CDW instability in the harmonic calculations is reminiscent of the effect of iso-valent and iso-electronic substitution of Se with lighter S. The harmonic calculation also predicts a CDW instability for NbS<sub>2</sub> that is not observed experimentally<sup>26</sup>.

Taken together, these facts indicate that for an ac-

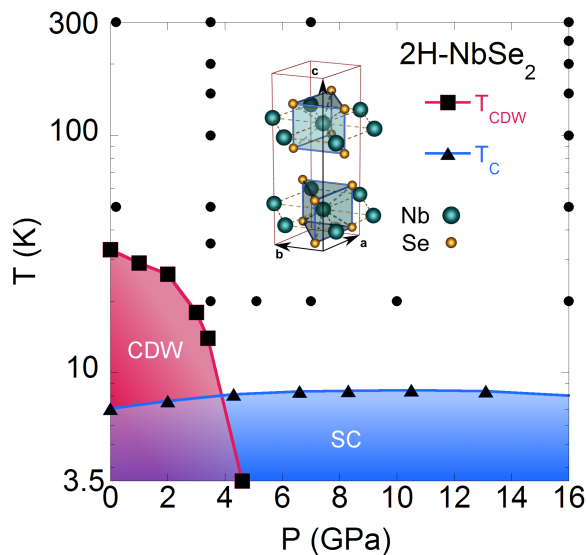


FIG. 1. Phase diagram of NbSe<sub>2</sub>. Squares indicate the limit of the CDW phase measured in Ref.<sup>12</sup> with the addition of the point at 4.6 GPa from Ref.<sup>11</sup>, triangles indicate the superconducting  $T_c$  measured in<sup>13</sup>, and circles indicate the pressure and temperature of our IXS measurements. Inset : crystallographic structure of 2H-NbSe<sub>2</sub><sup>1</sup>.

curate description of the ground state (even at  $T=0K$ ) of these systems, calculations beyond the standard harmonic approximation must be carried out. The impact of anharmonicity has recently been highlighted in different systems. To mention only a few, the thermodynamical properties of the metal-insulator transition in strongly correlated VO<sub>2</sub><sup>17</sup>, the transport properties of thermoelectric PbTe<sup>18</sup> or the electron-phonon interaction above the Verwey transition in magnetite Fe<sub>3</sub>O<sub>4</sub><sup>19</sup> are all strongly influenced by anharmonicity. Even at low temperatures, where its effects are expected to be weaker, it must be taken into account to explain the pressure dependence of the crystal structure of Calcium<sup>20</sup>, the inverse isotope effect in superconducting PdH<sup>21</sup>, or the phonon spectra at the proximity of the liquid-solid transition of Helium at 0K<sup>22</sup>. Finally, anharmonicity is crucial for understanding the ground state of a system when a quantum electronic phase transition coupled to the lattice occurs, as in e.g. ferroelectrics<sup>23</sup> or CDW compounds<sup>10,24-26</sup>. In most cases however, these effects are computationally too expensive to be evaluated in standard first-principle calculations, and therefore often disregarded.

Here, we report the investigation of the temperature and pressure dependence of the phonon spectra of NbSe<sub>2</sub> by using high resolution inelastic X-ray scattering (IXS) from a crystal in a diamond anvil cell, up to pressures as large as 16 GPa at  $T = 20$  K. We observe that the strong temperature dependence of the soft phonon mode is reduced by pressure, but still present even at 16 GPa.

We show that the temperature and pressure depen-

dence of the phonon spectra can be accurately accounted for when the effects of anharmonicity are explicitly included in the calculation. Anharmonic effects were calculated within the newly developed stochastic self-consistent harmonic approximation (SSCHA), yielding an unprecedented agreement with the experimentally determined temperature dependence of the phonon spectra at various pressures. We show that at low temperatures, for pressures between  $P_{CDW}$  and  $P_C$ , the CDW is destroyed by quantum fluctuations, which easily overcome the double-well lattice potential and, thus, are strongly affected by the anharmonic part of the potential. Surprisingly, we observe that anharmonic effects dominate the low-energy phonon spectrum of 2H-NbSe<sub>2</sub> in a large pressure range, extending at least up to 16 GPa  $\gg P_{CDW}$  and down to the lowest temperatures. Finally, we demonstrate that a large electron-phonon interaction, mostly due to optical modes rather than to the soft longitudinal acoustic mode which drives the CDW instability, contributes substantially to superconductivity in 2H-NbSe<sub>2</sub>, and naturally explains its insensitivity to the occurrence of a CDW.

## II. EXPERIMENT

Single crystals of 2H-NbSe<sub>2</sub> were grown using the vapor growth technique in sealed quartz tubes with iodine as a transport agent<sup>1</sup>. Typical dimensions of the crystals are  $100 \times 100 \times 50 \mu\text{m}^3$  ( $\vec{a} \times \vec{b} \times \vec{c}$ ). Pressure was generated using a diamond anvil cell, loaded with helium as a pressure transmitting medium to ensure highly hydrostatic conditions. Temperature was lowered using a custom-designed <sup>4</sup>He cryostat, and pressure was varied *in-situ* at low temperature using a helium-pressurized membrane. Each cell contained two rubies to monitor the pressure *in-situ* using the fluorescence technique. Measurements of the phonon dispersion of 2H-NbSe<sub>2</sub> were taken between room temperature and 20 K, and for pressures ranging from 0.2 to 16 GPa.

IXS measurements were carried out on beamline ID28 at the ESRF. The x-ray beam was aligned along the  $c$ -axis of the crystal. We used the (9,9,9) reflection on the backscattering monochromator with an incident energy of 17.794 keV, and a corresponding energy resolution of 1.3 meV HWHM (lorentzian fit of the elastic peak). The incident beam was focused by a multilayer mirror into a spot of  $100 \times 60 \mu\text{m}$  (width  $\times$  height). We used  $20 \times 60 \text{mm}$  (width  $\times$  height) slits at a 7 m distance giving a momentum resolution of  $0.014 \text{ \AA}^{-1}$  ( $a^* \times c^* \approx 2.1 \times 0.50 \text{ \AA}^{-1}$ ) in the (H,0,L) plane, and  $0.042 \text{ \AA}^{-1}$  ( $b^* \times \sin(60^\circ) \approx 1.8 \text{ \AA}^{-1}$ ) in the perpendicular direction. We measured the phonon dispersion along the  $\Gamma M$  direction close to  $\Gamma_{200}$  (*i. e.* (2-h, 0, 0)), where both longitudinal optical and acoustic like soft phonon branches can be observed. According to the balance of the dynamical structure factor of the 2 phonon modes and so of the inelastic scattering function  $S(\mathbf{q}, \omega)$ , the observation of one of the two branches can be

selected. For each transfer wave vector investigated, an energy scan up to 15meV was performed. All the spectra were fitted using the standard Levenberg-Marquadt algorithm, with the following free parameters : position and amplitude of the elastic peak; position, linewidth and amplitude of the phonon; and a constant background. We make the standard assumptions<sup>27,28</sup> that the elastic peak is Lorentzian, and that the phonon lineshape can be modeled by a damped harmonic oscillator convoluted by a normalized Lorentzian with a width corresponding to the resolution of the detector.

### III. ANHARMONIC CALCULATIONS

*Ab initio* calculations were performed within density functional perturbation theory and the generalized gradient approximation<sup>29</sup> making use of the QUANTUM ESPRESSO<sup>16</sup> code. An ultrasoft pseudopotential (norm-conserving) for Nb (Se), a 35Ry energy cutoff, and a  $24 \times 24 \times 8$  mesh for the electronic integrations were used. An Hermitian-Gaussian smearing of 0.01 Ry was used. Harmonic dynamical matrices were calculated within linear response in a grid of  $6 \times 6 \times 4$   $\mathbf{q}$  points. The stochastic self-consistent harmonic approximation (SSCHA)<sup>21,30</sup> calculations were performed using a  $3 \times 3 \times 1$  supercell, yielding anharmonic dynamical matrices in the commensurate  $3 \times 3 \times 1$  grid. The difference between the SSCHA dynamical matrices and the harmonic dynamical matrices in the  $3 \times 3 \times 1$  grid was Fourier interpolated to the points of the finer  $6 \times 6 \times 4$  grid. Adding the harmonic dynamical matrices in the  $6 \times 6 \times 4$  grid to the result of the interpolation, the SSCHA dynamical matrices in the finer  $6 \times 6 \times 4$  mesh were obtained. The experimental lattice parameters with relaxed internal coordinates were used.

The electron-phonon calculations were performed by using maximally localized Wannier functions<sup>31,32</sup> and interpolation of the electron-phonon matrix elements as in Ref.<sup>33</sup>. We used 14 Wannier functions (d-states of Nb and Se  $p_z$  states) and a  $6 \times 6 \times 4$  electron-momentum grid. We used the Fourier interpolated SSCHA dynamical matrices in the electron-phonon coupling calculations. The average electron-phonon coupling was interpolated using electron and phonon momentum grids of  $24 \times 24 \times 8$  randomly displaced from the origin.

## IV. RESULTS AND DISCUSSION

### A. Phonon spectra under pressure and anharmonicity

The temperature dependence of the low energy phonon dispersions recorded at pressures of 3.5 and 16 GPa are shown in Fig. 2 (some of the corresponding raw datas are shown in the supplementary materials). At  $T = 20$  K and  $P = 3.5$  GPa, the system is very close to the

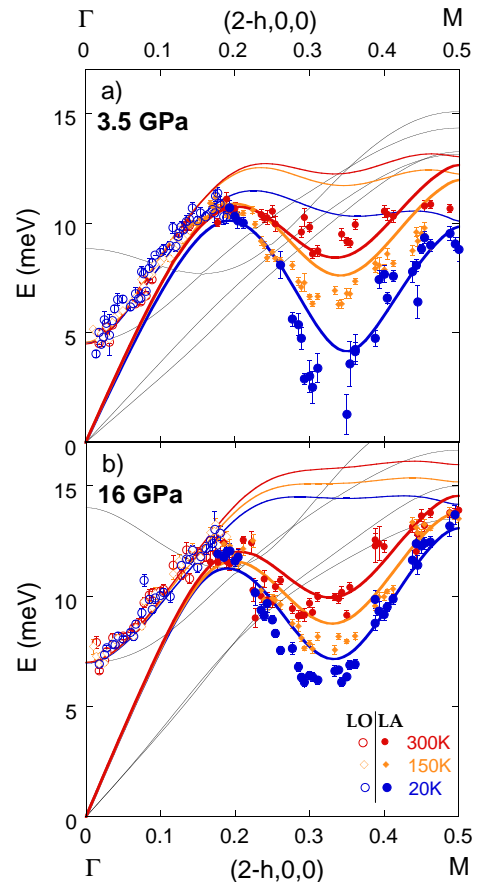


FIG. 2. Phonon dispersion at 3.5 GPa (a) and 16 GPa (b). Closed (resp. open) dots represent the experimentally determined longitudinal acoustic (longitudinal optical) soft phonon dispersions, and lines represent the results of phonon calculations. Close to the  $\Gamma$  point, the phonon dispersion shows clearly an optical branch. Closer to the M point, the energy of the phonon observed correspond to the acoustic like branch calculated. A tiny intensity excess at higher energy could be attributed to a second branch (see raw data on supplementary) but doesn't allow an accurate fit of the energy of the mode. Colored thick and thin lines represent the SSCHA results for the longitudinal acoustic and optical anharmonic phonons, respectively, at several temperatures. The thin black lines represent other phonon modes present in this energy range calculated within the SSCHA at 20 K, which are very harmonic and barely depend on temperature (see SI).

quantum critical regime reported in ref. 11. No particular enhancement of the elastic line intensity close to the CDW wavevector  $\mathbf{q}_{\text{CDW}} \approx (1.67, 0, 0)$  is observed. On the other hand, a colossal temperature dependent softening of the longitudinal acoustic phonon mode is seen : from  $\sim 9$  to  $\sim 1.5$  meV between room temperature and 20 K. While this mode is expected to condense around  $\sim 12$

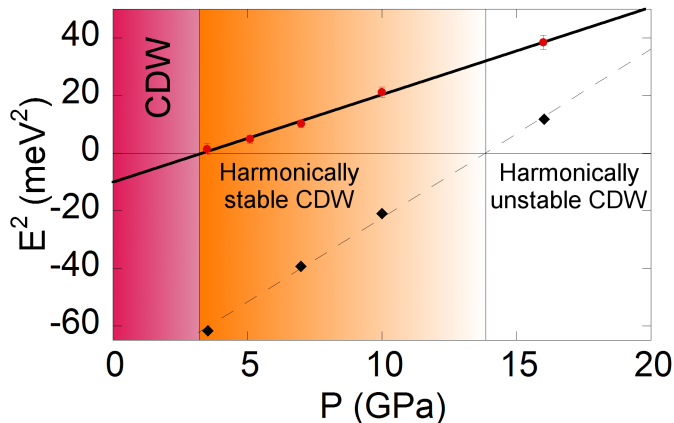


FIG. 3. Pressure dependence of the square of the measured energy of the longitudinal acoustic soft phonon at the CDW ordering wavevector and at 20 K (red dots) compared to the square of the energy calculated in the harmonic approximation (black diamonds). Lines are linear fits. The red region indicates the range of pressure where a CDW is observed experimentally at 20 K. The orange region indicates the range of pressure where harmonic calculations predict a CDW ground state.

K<sup>11</sup>, this temperature could not be reached at this pressure with the current experimental set-up. As we increase pressure to 16 GPa, the amplitude of the phonon softening is significantly reduced, but remains sizeable as the mode's energy almost decreases by a factor of 2 from 300 to 20 K. So far, most of the theoretical and experimental work on NbSe<sub>2</sub> has focused on the interplay between the electronic susceptibility and the electron-phonon interaction as possible mechanisms for the CDW formation<sup>34,35</sup>. The large temperature dependence indicates that strong anharmonic effects survive over a pressure range that is way larger than the experimentally reported CDW stability range ( $0 < P < P_{CDW}$ ) and might therefore play an important role that was up to now largely disregarded.

In Fig. 3, we plot the square of the soft phonon frequency measured at  $T = 20$  K at  $\mathbf{q}_{CDW}$  as a function of pressure. The linear dependence indicates that the mode hardens as  $\sqrt{P - P_{CDW}}$ . We also plot the square of the phonon frequency calculated within the harmonic approximation, which is negative - i.e. indicating that the system is unstable against CDW formation - up to 14 GPa  $\gg P_{CDW}$ . This is reminiscent of the situation encountered at ambient pressure in NbS<sub>2</sub>, where we have observed a large phonon softening upon cooling, insufficient however to induce the CDW formation despite the predictions of the harmonic ab-initio calculation<sup>26</sup>.

To quantify the effect of anharmonicity and check whether it is responsible for the destabilization of the

CDW between  $P_{CDW}$  and 14 GPa, we have carried out a series of calculations for the pressures and temperatures experimentally investigated, within the SSCHA approach<sup>21,30</sup> (see SI) which allows us to access directly the anharmonic free energy of the system, with full inclusion of the anharmonic potential terms.

The results are superimposed to our experimental dispersions in Fig. 2. Not only is the instability suppressed as experimentally observed, but the agreement between the measured and calculated dispersions over the entire pressure range is remarkable compared to harmonic ab-initio calculation. A tiny overestimation of phonon calculation is nevertheless observed in the range around  $\mathbf{q}_{CDW}$ . At finite temperature, anharmonicity usually manifests itself through the effect of many-body interactions between thermally excited phonons, henceforth limiting their lifetime. Surprisingly here, these effects are sufficient to suppress the CDW not only at finite temperature but also down to  $T = 0$  K between 4.6 and 14 GPa. This indicates that zero-point quantum fluctuations of the lattice are already strong enough to destroy the long range CDW order. This bears stark analogy with the destruction of long range magnetic order from spin-spin quantum fluctuations in low dimensional quantum magnets<sup>36</sup>.

Finally we note that these many-body effects are relevant not only at  $\mathbf{q} = \mathbf{q}_{CDW}$ , but extend up to the M point, the boundary of the Brillouin zone at  $\mathbf{q} = \mathbf{a}^*/2$ , where two low-energy modes, the longitudinal acoustic mode that drives the CDW transition and an optical mode, are substantially hardened with respect to the result of the harmonic calculation.

## B. Superconductivity

The importance of the electron-phonon interaction in the CDW formation has been emphasized<sup>10,34</sup>, but its role in superconductivity remains debated, as is, more generally, the interplay between these two orders. Indeed, the absence of reliable ab initio phonon calculations in the high symmetry phase, has prevented a calculation of the superconducting critical temperature. Having achieved a detailed understanding of the low energy part of the experimental phonon spectra and having shown how anharmonicity can suppress the long range ordered CDW phase, we can now address the superconducting properties of NbSe<sub>2</sub> by calculating the Eliashberg function and the integrated electron-phonon coupling (see SI) as a function of pressure. As of now, this calculation can only be done in the high pressure phase, where the number of atoms per unit cell is low enough. We show in Fig. 4 the results of the calculation at 7 GPa (data for other pressures are shown in the SI). We find that the average electron-phonon coupling is as large as  $\lambda = 1.16$  (see Tab. I for other pressures), demonstrating that NbSe<sub>2</sub> is a strong coupling superconductor.

Previous works<sup>9,10,14,15,37</sup> identified the large electron-phonon coupling of the soft acoustic mode at  $\mathbf{q}_{CDW}$  as

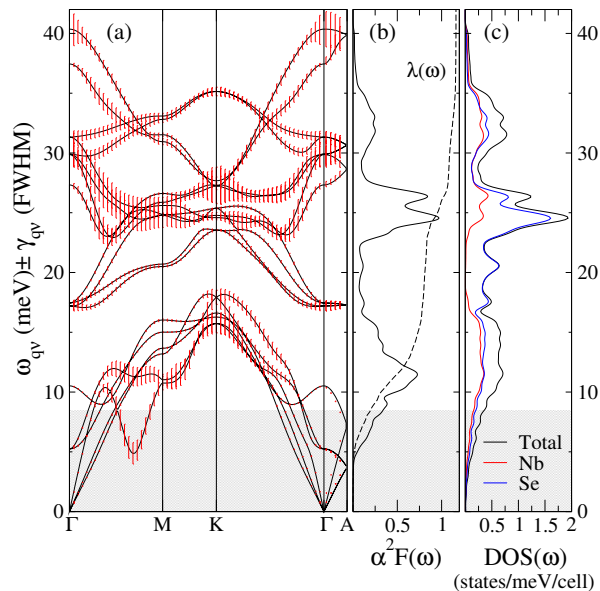


FIG. 4. (a) Calculated phonon dispersion at 7 GPa and 0 K with the SSCHA. The size of the bars is proportional to the electron-phonon contribution to the phonon linewidth (the bar is twice the FWHM). (b) The Eliashberg function  $\alpha^2F(\omega)$  and the integrated electron-phonon coupling  $\lambda(\omega)$ . (c) The phonon density of states decomposed into the different atoms. In all figures the grey background denotes the integration area used to infer that the soft acoustic longitudinal mode contributes 17% of the total electron-phonon coupling.

P (GPa)	$\lambda$	$\omega_{log}$ (meV)	$T_c$ calc. (K)	$T_c$ exp. (K)
3.5	1.28	12.6	11.3	7.8
7	1.16	13.7	10.5	8.2
16	0.91	16.4	7.8	7.8

TABLE I. Calculated  $\lambda$ , logarithmic frequency average  $\omega_{log}$ , and  $T_c$  values for 2H-NbSe<sub>2</sub> at 3.5, 7 and 16 GPa. The McMillan equation with  $\mu^* = 0.16$  is used to calculate  $T_c$ . Experimental data are taken from Ref.<sup>13</sup>.

the mechanism responsible for the CDW formation. For this reason, it is natural to expect that this soft mode also plays a key role in superconductivity. However, its contribution to the average electron-phonon coupling is less than 17% (as it can be inferred from the integrated  $\lambda(\omega)$  in Fig. 4), meaning that it has only a marginal role in superconductivity. Indeed, the strong coupling of this mode is very localized around  $\mathbf{q}_{CDW}$ , and its contribution to  $\lambda$  averages out when integrating over the Brillouin

zone. The modes sustaining superconductivity are given by the two main contributions to the Eliashberg function: a broad peak centred around  $\approx 11.5$  meV and a second one in the 22 – 26 meV region. These two features contribute to  $\approx 70\%$  of the total electron-phonon coupling. Further insights are obtained by decomposing the phonon density of states (DOS) in atomic vibrations along different directions. As the DOS and  $\alpha^2F(\omega)$  are very similar, the decomposition will also apply to the Eliashberg function. The low energy feature at 11.5 meV is mainly due to Nb and Se vibrations parallel to the Nb plane, corresponding to the flat phonon band along  $\Gamma M$  suffering from a large anharmonic correction, while the features in the 22 – 26 meV range are mostly attributed to out-of-plane and in-plane Se displacements with a non negligible Nb component. In both modes sustaining superconductivity there is a substantial Se component, upturning the conventional wisdom that in superconducting dichalcogenides the chalcogene is accessory while the transition metal plays a key role<sup>2</sup>. Our work demonstrates that the superconducting properties strongly depend on both the transition metal and the chalcogene, offering a natural explanation for the different relation between CDW and superconductivity encountered in different dichalcogenides<sup>38–40</sup>. Moreover, as optical phonon modes contribute strongly to superconductivity in 2H-NbSe<sub>2</sub>, while the CDW is determined by the softening of the longitudinal acoustic mode, the superconducting  $T_c$  is insensitive to the presence of the CDW, explaining the phase diagram in Fig. 1.

## V. OUTLOOK

On a more general basis, our work points toward the key role of anharmonicity in destroying the CDW order by quantum and thermal phonon-fluctuations. This evidence calls for a rewriting of the paradigmatic analysis of CDW instabilities based on the competition between electron fluctuations (Fermi surface effects) and the electron-phonon interaction<sup>24</sup>. Our results, in this respect, are fundamental and relevant for a very large set of materials exhibiting a CDW instability - or more generally a second order electronic quantum phase transition coupled to the lattice - such as transition metal dichalcogenides, cuprates<sup>41,42</sup>, Bechgaard salts and transition metal bronzes.

## VI. REFERENCES

\* [m.leroux@anl.gov](mailto:m.leroux@anl.gov); Present address : Materials Science Division, Argonne National Laboratory, 9700 S. Cass Avenue, Argonne, Illinois 60439, USA

† [matteo.calandra@upmc.fr](mailto:matteo.calandra@upmc.fr)

‡ [pierre.rodriere@neel.cnrs.fr](mailto:pierre.rodriere@neel.cnrs.fr)

- <sup>1</sup> Moncton, D. E., Axe, J. D. & DiSalvo, F. J. Neutron scattering study of the charge-density wave transitions in 2H-NbSe<sub>2</sub> and 2H-TaSe<sub>2</sub> by Neutron Scattering. *Phys. Rev. B* **16**, 801-819 (1975).
- <sup>2</sup> Wilson J.A., DiSalvo F. J., Mahajan S. Charge-density waves and superlattices in the metallic layered transition metal dichalcogenides *Adv. Phys.* **24** (1975) 117-201
- <sup>3</sup> Yokoya, T., Kiss, T., Chainani, A., Shin, S., Nohara, M. and Takagi, H., *Science* **294** 2518 (2001).
- <sup>4</sup> T. Valla, A. V. Fedorov, P. D. Johnson, P.-A. Glans, C. McGuinness, K. E. Smith, E. Y. Andrei, and H. Berger, *Phys. Rev. Lett.* **92**, 086401 (2004)
- <sup>5</sup> T. Kiss, T. Yokoya, A. Chainani, S. Shin, T. Hanaguri, M. Nohara, and H. Takagi, *Nat. Phys.* **3**, 720 (2007).
- <sup>6</sup> I. Guillamon, H. Suderow, F. Guinea, and S. Vieira, Intrinsic atomic-scale modulations of the superconducting gap of 2H-NbSe<sub>2</sub>. *Phys. Rev. B* **77** 134505 (2008)
- <sup>7</sup> S. V. Borisenko, A. A. Kordyuk, V. B. Zabolotnyy, D. S. Inosov, D. Evtushinsky, B. Büchner, A. N. Yaresko, A. Varykhalov, R. Follath, W. Eberhardt, L. Patthey, and H. Berger, *Phys. Rev. Lett.* **102**, 166402 (2009).
- <sup>8</sup> D. J. Rahn, D. J., Hellmann, S., Kalläne, M., Sohr, C., Kim, T. K., Kipp, L. and Rossnagel, K. Gaps and kinks in the electronic structure of the superconductor 2H-NbSe<sub>2</sub> from angle-resolved photoemission at 1 K *Phys. Rev. B* **85**, 224532 (2012)
- <sup>9</sup> Arguello, C. J., Rosenthal, E. P., Andrade, E. F. et al. Quasiparticle Interference Quasiparticle Interactions and the Origin of the Charge Density Wave in 2H-NbSe<sub>2</sub> *Phys. Rev. Lett.* **114**, 037001 (2015)
- <sup>10</sup> Weber, F. et al. Extended Phonon Collapse and the Origin of the Charge-Density Wave in 2H-NbSe<sub>2</sub>. *Phys. Rev. Lett.* **107**, 107403 (2011).
- <sup>11</sup> Feng Y. et al. Order parameter fluctuations at a buried quantum critical point *Proceedings of the National Academy of Sciences* **109**, 7224-7229 (2012).
- <sup>12</sup> Berthier C., Molinié P., Jérôme D., Evidence for a connection between charge density waves and pressure enhancement of superconductivity in 2H-NbSe<sub>2</sub> *Solid State Communications* **18**, 1393-1395 (1976).
- <sup>13</sup> Suderow, H., Tissen, V. G., Brison, J. P., Martínez, J. L., Vieira, S. Pressure induced effects on the fermi surface of superconducting 2H-NbSe<sub>2</sub>, *Phys. Rev. Lett.* **95**, 117006 (2005).
- <sup>14</sup> Calandra, M., Mazin, I. I. & Mauri, F. Effect of dimensionality on the charge-density wave in few-layer 2H-NbSe<sub>2</sub>. *Phys. Rev. B* **80**, 241108 (2009).
- <sup>15</sup> Weber, F., et al. Optical phonons and the soft mode in 2H-NbSe<sub>2</sub>. *Phys. Rev. B* **87**, 245111 (2013).
- <sup>16</sup> Giannozzi et al. QUANTUM ESPRESSO: a modular and open-source software project for quantum simulations of materials. *J. Phys. Condens. Matter* **21**, 395502 (2009).
- <sup>17</sup> Budai, J. D. et al. Metallization of Vanadium dioxide driven by large phonon entropy. *Nature* **515**, 535-539 (2014).
- <sup>18</sup> Delaire, O. et al. Giant anharmonic phonon scattering in PbTe. *Nat. Mat.* **10**, 614-619 (2011).
- <sup>19</sup> Hoesch, M. et al. Anharmonicity due to Electron-Phonon Coupling in Magnetite. *Phys. Rev. Lett.* **110**, 207204 (2013).
- <sup>20</sup> Errea, I., Rousseau, B. & Bergara, A. Anharmonic Stabilization of the High-Pressure Simple Cubic Phase of Calcium. *Phys. Rev. Lett.* **106**, 165501 (2011).
- <sup>21</sup> Errea, I., Calandra, M. & Mauri, F. First-Principles Theory of Anharmonicity and the Inverse Isotope Effect in Superconducting Palladium-Hydride Compounds. *Phys. Rev. Lett.* **111**, 177002 (2013).
- <sup>22</sup> Glyde, H. R. Excitations in liquid and solid Helium. Clarendon Press, Oxford 1994
- <sup>23</sup> Rowley, S. E. et al. Ferroelectric quantum criticality *Nat. Phys.* **10**, 367-372 (2014).
- <sup>24</sup> Grüner, G., Density Waves in Solids, Edited by Perseus Books (2000)
- <sup>25</sup> Varma, C. M. & Simons, A. L. Strong-Coupling Theory of Charge-Density-Wave Transitions. *Phys. Rev. Lett.* **51**, 138-141 (1983).
- <sup>26</sup> Leroux, M. et al. Anharmonic suppression of charge density waves in 2H-NbS<sub>2</sub>. *Phys. Rev. B* **86**, 155125 (2012).
- <sup>27</sup> Fåk, B., Dorner, B. Phonon line shapes and excitation energies *Physica B: Condensed Matter* **234-236**, 1107-1108 (1997)
- <sup>28</sup> Burkel, E. Phonon spectroscopy by inelastic x-ray scattering. *Reports on Progress in Physics* **63**, 171-232 (2000)
- <sup>29</sup> Perdew, J. P., Burke, K., Ernzerhof, M. Generalized gradient approximation made simple *Phys. Rev. Lett.* **77**, 3865-3868 (1996)
- <sup>30</sup> Errea, I., Calandra M., Mauri F. Anharmonic free energies and phonon dispersions from the stochastic self-consistent harmonic approximation: Application to platinum and palladium hydrides. *Phys. Rev. B* **89**, 064302 (2014).
- <sup>31</sup> Marzari, N., Vanderbilt, D. Maximally localized generalized Wannier functions for composite energy bands. *Phys. Rev. B* **56**, 12847-12865 (1997)
- <sup>32</sup> Souza, I., Marzari, N., Vanderbilt, D. Maximally localized Wannier functions for entangled energy bands *Phys. Rev. B* **65**, 035109 (2002)
- <sup>33</sup> Calandra, M., Profeta, G., Mauri, F. Adiabatic and non-adiabatic phonon dispersion in a Wannier function approach *Phys. Rev. B* **82**, 165111 (2010)
- <sup>34</sup> Johannes, M. D., Mazin, I. I. & Howells, C. A. Fermi-surface nesting and the origin of the charge-density wave in NbSe<sub>2</sub>. *Phys. Rev. B* **73**, 205102 (2006).
- <sup>35</sup> X. Zhu, Y. Cao, J. Zhang, E. W. Plummer, Classification of charge density waves based on their nature *Proc. Nat. Ame. Soc.* **112** 2367 (2015)
- <sup>36</sup> Balents, L. Spin liquids in frustrated magnets. *Nature* **464**, 199-208 (2010).
- <sup>37</sup> Gor'kov, L. P. Strong electron-lattice coupling as the mechanism behind charge density wave transformations in transition-metal dichalcogenides. *Phys. Rev. B* **85**, 165142 (2012) and references therein.
- <sup>38</sup> Tissen V. G., et al. Pressure dependence of superconducting critical temperature and upper critical field of 2H-NbS<sub>2</sub> *Phys. Rev. B* **87**, 134502 (2013)
- <sup>39</sup> Kusmartseva, S. B., Berger, H., Forró, L., Tutis, E. Pressure Induced Superconductivity in Pristine 1T-TiSe<sub>2</sub> *Phys. Rev. Lett.* **103**, 236401 (2009)
- <sup>40</sup> S. B. S. Kusmartseva, A. F., Akrap, A., Berger H., Forro, L., Tutis, E. From Mott state to superconductivity in 1T-TaS<sub>2</sub> *Nat Mater* **7** 960-965 (2008)
- <sup>41</sup> Ghiringhelli, G. et al. Long-Range Incommensurate Charge Fluctuations in (Y,Nd)Ba<sub>2</sub>Cu<sub>3</sub>O<sub>6+x</sub>. *Science* **337**, 821-825 (2012).
- <sup>42</sup> Le Tacon, M. et al. Inelastic X-ray scattering in YBa<sub>2</sub>Cu<sub>3</sub>O<sub>6.6</sub> reveals giant phonon anomalies and elastic central peak due to charge-density-wave formation. *Nat. Phys.* **10**, 52-58 (2014).

## VII. ACKNOWLEDGEMENTS

Sabrina Salmon-Bourmand is thanked for her help in the synthesis of 2H-NbSe<sub>2</sub> single crystals. P.R. and M.L. acknowledge financial support from the French National Research Agency through Grant No. ANR-12-JS04-0003-01 SUBRISSYME. M.C, F.M. and I.E. acknowledge support from the Basque Government (Grant No. BFI-2011-65), Spanish Ministry of Economy and Competitiveness (FIS2013-48286-C2-2-P,) Graphene Flagship and ANR (contract ANR-13-IS10-0003-01) and Prace (2014102310). Calculations were performed at IDRIS, CINES, DIPC and at CEA TGCC.

## VIII. AUTHOR CONTRIBUTIONS

- Maxime Leroux, Mathieu Le Tacon, Sofia-Michaela Souliou, Gaston Garbarino, Laurent Cario, Alexey

Bosak and Pierre Rodière performed the IXS measurements.

- Ion Errea, Matteo Calandra and Francesco Mauri carried out the calculations.
- Laurent Cario supervised the synthesis and characterisation of single crystals of 2H-NbSe<sub>2</sub>.

## IX. COMPETING FINANCIAL INTERESTS STATEMENT

The authors declare no competing financial interests.